

Personal pdf file for

Tawit Suriyo, Nanthanit Pholphana, Nuchanart Rangkadilok,
Apinya Thiantanawat, Piyajit Watcharasit,
Jutamaad Satayavivad

With compliments of Georg Thieme Verlag

www.thieme.de

Andrographis paniculata Extracts
and Major Constituent Diterpenoids
Inhibit Growth of Intrahepatic
Cholangiocarcinoma Cells by
Inducing Cell Cycle Arrest and
Apoptosis

DOI 10.1055/s-0034-1368399

Planta Med 2014; 80: 533–543

For personal use only.
No commercial use, no depositing in repositories.

Publisher and Copyright:

© 2014 by
Georg Thieme Verlag KG
Rüdigerstraße 14
70469 Stuttgart
ISSN 0032-0943

Reprint with the
permission by
the publisher only

 **Thieme**

Andrographis paniculata Extracts and Major Constituent Diterpenoids Inhibit Growth of Intrahepatic Cholangiocarcinoma Cells by Inducing Cell Cycle Arrest and Apoptosis

Authors

Tawit Suriyo¹, Nanthanit Pholphana¹, Nuchanart Rangkadilok^{1,2}, Apinya Thiantanawat^{1,2}, Piyajit Watcharasit^{1,2}, Jutamaad Satayavivad^{1,2,3}

Affiliations

¹ Laboratory of Pharmacology, Chulabhorn Research Institute, Bangkok, Thailand

² Chulabhorn Graduate Institute, Bangkok, Thailand

³ Center of Excellence on Environmental Health and Toxicology, Office of Higher Education Commission, Ministry of Education, Bangkok, Thailand

Key words

- *Andrographis paniculata*
- Acanthaceae
- andrographolide
- cholangiocarcinoma
- bile duct cancer
- apoptosis
- cell cycle arrest

Abstract

Andrographis paniculata is an important herbal medicine widely used in several Asian countries for the treatment of various diseases due to its broad range of pharmacological activities. The present study reports that *A. paniculata* extracts potently inhibit the growth of liver (HepG2 and SK-Hep1) and bile duct (HuCCA-1 and RMCCA-1) cancer cells. *A. paniculata* extracts with different contents of major diterpenoids, including andrographolide, 14-deoxy-11,12-didehydroandrographolide, neoandrographolide, and 14-deoxyandrographolide, exhibited a different potency of growth inhibition. The ethanolic extract of *A. paniculata* at the first true leaf stage, which contained a high amount of 14-deoxyandrographolide but a low amount of andrographolide, showed a cytotoxic to cancer cells about 4 times higher than the water extract of *A. paniculata* at the mature leaf stage, which contained a high amount of andrographolide but a low amount of 14-deoxyandrographolide. Andrographolide, not 14-deoxy-11,12-didehydroandrographolide, neoandrographolide, or 14-deoxyandrographolide, possessed potent cytotoxic activity against the growth of liver and bile duct cancer cells. The cytotoxic effect of the water extract of *A. paniculata* at the mature leaf stage could be explained by the present amount of andrographolide, while the cytotoxic effect of the ethanolic extract of *A. paniculata* at the first true leaf stage could not. HuCCA-1 cells showed more sensitivity to *A. paniculata* extracts and andrographolide

than RMCCA-1 cells. Furthermore, the ethanolic extract of *A. paniculata* at the first true leaf stage increased cell cycle arrest at the G0/G1 and G2/M phases, and induced apoptosis in both HuCCA-1 and RMCCA-1 cells. The expressions of cyclin-D1, Bcl-2, and the inactive proenzyme form of caspase-3 were reduced by the ethanolic extract of *A. paniculata* in the first true leaf stage treatment, while a proapoptotic protein Bax was increased. The cleavage of poly (ADP-ribose) polymerase was also found in the ethanolic extract of *A. paniculata* in the first true leaf stage treatment. This study suggests that *A. paniculata* could be a promising herbal plant for the alternative treatment of intrahepatic cholangiocarcinoma.

Abbreviations

AP ₁ :	andrographolide
AP ₃ :	14-deoxy-11,12-didehydroandrographolide
AP ₄ :	neoandrographolide
AP ₆ :	14-deoxyandrographolide
COX-2:	cyclooxygenase 2
FTLEE:	ethanolic extract of the first true leaf of <i>A. paniculata</i>
MLWE:	water extract of the mature leaf of <i>A. paniculata</i>
PS:	phosphatidylserine
PI:	propidium iodide
P/S:	penicillin/streptomycin
PARP:	poly (ADP-ribose) polymerase

received February 5, 2014
revised March 3, 2014
accepted March 17, 2014

Bibliography

DOI <http://dx.doi.org/10.1055/s-0034-1368399>
Published online April 29, 2014
Planta Med 2014; 80: 533–543
© Georg Thieme Verlag KG
Stuttgart · New York ·
ISSN 0032-0943

Correspondence

Assoc. Prof. Dr. Jutamaad Satayavivad

Laboratory of Pharmacology
Chulabhorn Research Institute
54 Kamphaeng Phet 6 Rd.
Laksi, Bangkok 10210
Thailand
Phone: + 66 25 53 85 55
ext. 85 39
Fax: + 66 25 53 85 62
jutamaad@cri.or.th

Introduction

Andrographis paniculata (Burm.f.) Nees (Acanthaceae), generally known as “King of Bitters”, is an important traditional herbal medicine widely used for the treatment of various diseases such

as respiratory infection, inflammation, cold, fever, bacterial dysentery, and diarrhea in many Asia and Southeast Asia countries, including China, India, and Thailand [1]. *A. paniculata* has a broad range of pharmacological beneficial properties, for example, anti-inflammatory, immunostimula-

tory, antidiarrheal, antiviral, antimalaria, hepatoprotective, cardioprotective, hypoglycemic, and anticancer activities [2,3]. Phytochemical investigations of the aerial parts of *A. paniculata* revealed the presence of a large number of diterpenoids, including AP₁, AP₃, AP₄, and AP₆ [4]. The chemical structures of these diterpenoids are shown in **Fig. 1**. These diterpenoids exhibit different pharmacological activities. AP₁ showed strong anti-inflammatory and anticancer properties [3,5]. Our previous studies demonstrated that AP₃ had a potent hypotensive property [6] and antiplatelet activity [7]. Furthermore, AP₄ showed anti-infective and anti-hepatotoxic activities, while AP₆ showed immunomodulatory and anti-atherosclerotic activities [8]. Our recent study indicated the changes in the content of these four active diterpenoids at different plant growth stages of *A. paniculata*. AP₁ is found at the highest level in leaves at vegetative and seed-forming stages, while AP₆ is found at the highest level in leaves at first true leaf and transferring stages [9]. Therefore, *A. paniculata* extracts obtained at different plant growth stages may exert their pharmacological activities differently.

Cholangiocarcinoma is regarded as inclusive of intrahepatic, perihilar, and distal extrahepatic tumors of the bile ducts epithelium. It is a relatively rare type of primary liver cancer but high incidence rates have been reported in Southeast Asia, especially Thailand [10,11]. Notably, recent epidemiological studies have shown that the incidence and mortality rates of cholangiocarcinoma are increasing globally [12,13]. The treatment of cholangiocarcinoma is challenging as the tumor is an aggressive malignancy typified by poor prognosis and unresponsiveness to radio- or chemotherapies [14,15]. Therefore, an alternative effective treatment of cholangiocarcinoma is urgently needed.

Presently, there is a renewed interest in the search for anticancer agents from medicinal herbs because they may prove to be a major source of new and innovative drugs. *A. paniculata* and its major constituent diterpenoids, especially AP₁, have been shown to have anticancer activity in both *in vitro* and *in vivo* experimental models of various types of cancer [3]. However, there is no study of *A. paniculata* or its major constituent diterpenoids against cholangiocarcinoma. In the present study, we report the growth inhibitory effect of *A. paniculata* extracts at different plant growth stages and its major constituent diterpenoids, including AP₁, AP₃, AP₄, and AP₆, on liver and bile duct cancer cells.

Results

The extracts of *A. paniculata* at different plant growth stages were prepared, and the contents of AP₁, AP₃, AP₄, and AP₆ in the extracts were determined by HPLC-DAD. The results showed that *A. paniculata* extracts contained different amount of diterpenoids (**Fig. 2**). For MLWE, the contents of AP₁, AP₃, AP₄, and AP₆ were 8.26, 0.62, 6.34, and 2.20 mg/g dry weight, respectively (**Table 1**). Meanwhile, the contents of AP₁, AP₃, AP₄, and AP₆ in FTLEE were 0.59, 5.74, 8.82, and 123.73 mg/g dry weight, respectively. Notably, the content of AP₁ in MLWE was 14 times higher than in FTLEE, while the contents of AP₃ and AP₆ in MLWE were 9.3 and 56.2 times lower than in FTLEE, respectively.

Since both MLWE and FTLEE contained different contents of the major diterpenoids, next we investigated the cancer growth inhibiting effects of the extracts. The cytotoxic effects of MLWE and FTLEE on hepatocellular carcinoma (HepG2 and SK-Hep1) and intrahepatic cholangiocarcinoma (HuCCA-1 and RMCCA-1) cell lines were evaluated by the MTT assay. The results demon-

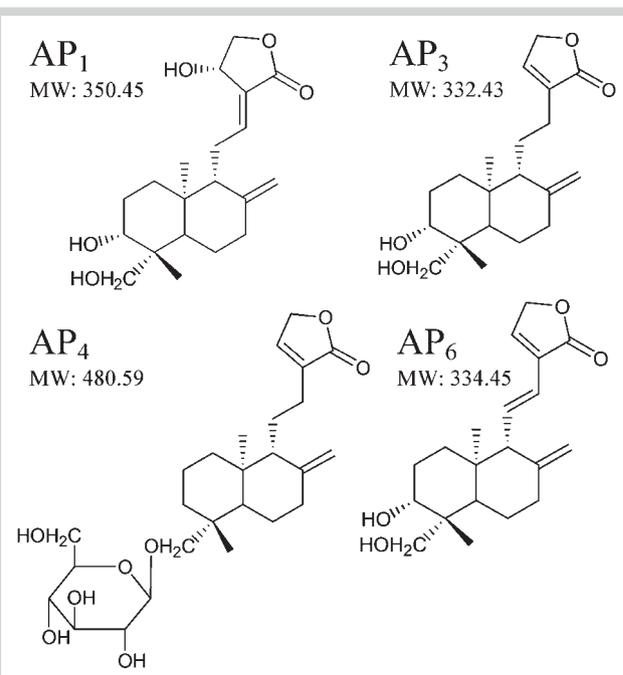


Fig. 1 Chemical structures of major constituent diterpenoids of *Andrographis paniculata*. AP₁: andrographolide; AP₃: 14-deoxy-11,12-didehydroandrographolide; AP₄: neoandrographolide; AP₆: 14-deoxyandrographolide; MW: molecular weight.

strated that FTLEE exhibited cytotoxic effects to all tested cell lines about 4 times higher than MLWE (**Fig. 3**). The IC₅₀ values (the concentration that inhibited 50% growth) of MLWE at 24 h treatment in HepG2, SK-Hep1, HuCCA-1, and RMCCA-1 were 3.9, 2.6, 1.6, and 3.2 mg/mL, respectively (**Table 2**). Moreover, the IC₅₀ values of FTLEE at 24 h treatment in HepG2, SK-Hep1, HuCCA-1, and RMCCA-1 were 0.96, 0.55, 0.40, and 0.72 mg/mL, respectively. It should be noted that HuCCA-1 was the most sensitive cell line to both MLWE and FTLEE followed by SK-Hep1, RMCCA-1, and HepG2, respectively. Indeed, the IC₅₀ values of both *A. paniculata* extracts in HuCCA-1 cells were about 2 times lower than in RMCCA-1 cells.

Previous results revealed that *A. paniculata* extracts at the different growth stages, which consisted of different contents of diterpenoids, showed different effects on cancer cells. Next, we further investigated the cytotoxic effects of pure AP₁, AP₃, AP₄, and AP₆ on hepatocellular carcinoma and intrahepatic cholangiocarcinoma cells. The results indicated that the cytotoxic potency of AP₁ was higher than AP₃, AP₄, and AP₆ (**Fig. 4**). The IC₅₀ values of AP₁ at 24 h treatment in HepG2, SK-Hep1, HuCCA-1, and RMCCA-1 were 90.63, 47.74, 29.26, and 52.57 μM, respectively (**Table 3**). Furthermore, the IC₅₀ values of the other pure diterpenoids, including AP₃, AP₄, and AP₆ in HepG2, SK-Hep1, HuCCA-1, and RMCCA-1, were found to be higher than 100, 100, 100, and 1000 μM, respectively. Note that gemcitabine (positive control) concentration-dependently decreased cell viability. These results suggested that AP₁ possessed a potent cytotoxic activity against the growth of hepatocellular carcinoma and intrahepatic cholangiocarcinoma cells, while AP₃, AP₄, and AP₆ showed a low or non-cytotoxic property against these cancer cell growths.

To correlate the cytotoxic effects of *A. paniculata* extracts with the content of each diterpenoid present in the extracts, the con-

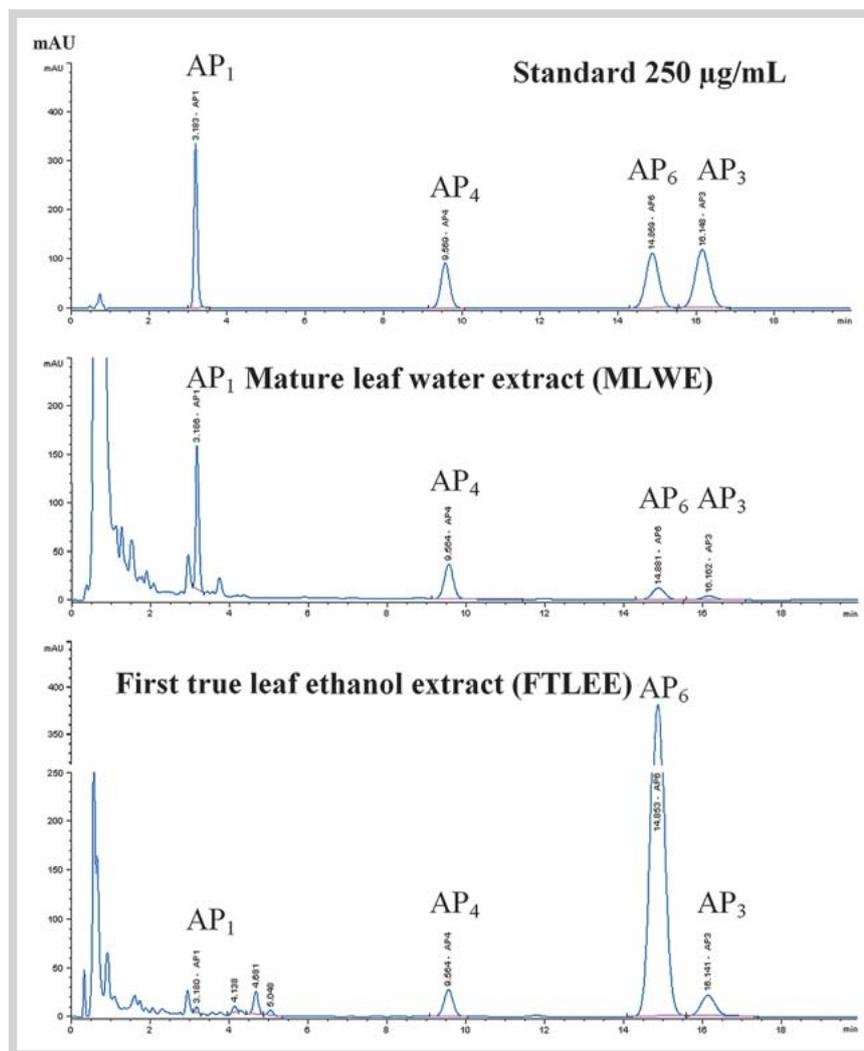


Fig. 2 Representative chromatograms of the major constituent diterpenoids of *Andrographis paniculata* extracts. AP₁: andrographolide; AP₃: 14-deoxy-11,12-didehydroandrographolide; AP₄: neoandrographolide; AP₆: 14-deoxyandrographolide. (Color figure available online only.)

<i>Andrographis paniculata</i> extracts	Diterpenoids (mg/g dry weight)			
	AP ₁	AP ₃	AP ₄	AP ₆
Mature leaf water extract	8.26 ± 0.02	0.62 ± 0.00	6.34 ± 0.02	2.20 ± 0.01
First true leaf ethanol extract	0.59 ± 0.02	5.74 ± 0.05	8.82 ± 0.02	123.73 ± 0.19

Table 1 Contents of the major constituent diterpenoids of *Andrographis paniculata* extracts.

AP₁: andrographolide; AP₃: 14-deoxy-11,12-didehydroandrographolide; AP₄: neoandrographolide; AP₆: 14-deoxyandrographolide

centration of each diterpenoid in the *A. paniculata* extracts for the IC₅₀ value was calculated and then compared to the IC₅₀ value of each pure diterpenoid. The results showed that the concentration of AP₁ in MLWE in HepG2, SK-Hep1, HuCCA-1, and RMCCA-1 cells had IC₅₀ values of 91.92, 61.28, 37.71, and 75.42 µM, respectively (● **Table 4**). Note that these concentrations of AP₁ in MLWE for the IC₅₀ values were very close and correlated well with the IC₅₀ value of AP₁ in the same cell lines (● **Table 3**), while the concentrations of AP₃, AP₄, and AP₆ in the MLWE had IC₅₀ values far lower than the IC₅₀ values of each pure diterpenoid. Furthermore, the concentrations of all four diterpenoids in FTLEE had IC₅₀ values far lower than the IC₅₀ values of each pure diterpenoid. These results suggested that the cytotoxic effect of MLWE could be explained by the present amount of AP₁, while the cytotoxic effect of FTLEE could not be explained by the present amounts of AP₁, AP₃, AP₄, or AP₆.

Since FTLEE showed a potent cytotoxic effect to intrahepatic cholangiocarcinoma cells, we then determined the effects of FTLEE on the cell cycle of HuCCA-1 and RMCCA-1 cells. The cells were incubated with different cytotoxic concentrations (0.2–1.2 mg/mL) of FTLEE for 24 h. Cell cycles were measured by flow cytometry with PI staining. The results showed that FTLEE concentration-dependently decreased the percentage of cells in the S phase in both HuCCA-1 and RMCCA-1 cells (● **Fig. 5**). The percentage of HuCCA-1 cells in the S phase decreased from 37.46% for the control to 21.86% for cells treated with 0.8 mg/mL of FTLEE. Furthermore, the percentage of RMCCA-1 cells in the S phase decreased from 37.84% for the control to 20.17% for cells treated with 1.2 mg/mL of FTLEE. The decrease of cells in the S phase was accompanied with a significantly increased percentage of cells in the G₀/G₁ and G₂/M phases. Notably, the positive control (100 µM of etoposide) completely decreased the percentage of cells in the S phase

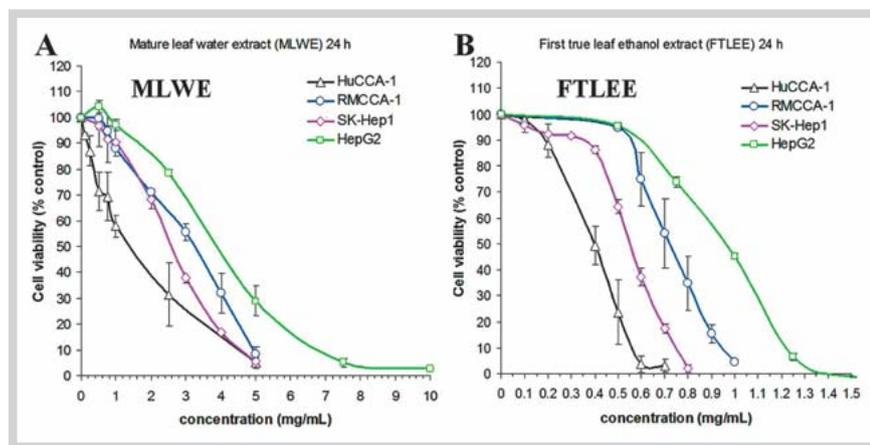


Fig. 3 Effects of *Andrographis paniculata* extracts on hepatocellular carcinoma (HepG2 and SK-Hep1) and intrahepatic cholangiocarcinoma (HuCCA-1 and RMCCA-1) cell viability. Cells were treated with (A) 0.1–10 mg/mL of MLWE or (B) 0.1–1.5 mg/mL of FTLEE for 24 h. Cell viability was assessed by the MTT assay. Each data point represents the mean \pm standard error of three independent experiments and is expressed relative to the control. (Color figure available online only.)

<i>Andrographis paniculata</i> extracts	IC ₅₀ value at 24 h treatment (mg/mL)			
	Hepatocellular carcinoma		Cholangiocarcinoma	
	HepG2	SK-Hep1	HuCCA-1	RMCCA-1
Mature leaf water extract	3.9	2.6	1.6	3.2
First true leaf ethanol extract	0.96	0.55	0.40	0.72

Table 2 Calculated IC₅₀ values of *Andrographis paniculata* extracts in hepatocellular carcinoma and intrahepatic cholangiocarcinoma cells.

and dramatically increased the percentage of cells in the G2/M phase. Since unattached floating cells were removed by the medium removal step before PI staining, the percentage of cells in the sub-G1 phase, which are the fragmented DNA cells and represent the late stage of apoptosis, showed no difference among the groups after treatment with FTLEE or even in the positive control etoposide. These results suggested that the FTLEE of *A. paniculata* induced cell cycle arrest at the G0/G1 and G2/M phases in intrahepatic cholangiocarcinoma cells.

In order to further study whether the loss of cell viability induced by FTLEE was associated with apoptosis, we then determined the death mechanism of FTLEE in both HuCCA-1 and RMCCA-1 cells. Apoptosis is characterized by various biochemical features including PS externalization to the cell surface, which can be determined by an annexin V-FITC apoptosis detection kit. Cells were incubated with different cytotoxic concentrations (0.2–1.0 mg/mL) of FTLEE for 24 h, and then the cells were analyzed for apoptosis and necrosis by flow cytometry with annexin V/PI dual staining. The results demonstrated that FTLEE induced apoptotic cell death in a concentration-dependent manner in both HuCCA-1 and RMCCA-1 cells (Fig. 6). In HuCCA-1 cells, 7.9–37.8% of apoptotic cells resulted from the treatment of FTLEE at 0.2–0.8 mg/mL, while only 5.5% of cells underwent apoptosis in the control (Fig. 6B). In RMCCA-1 cells, 10.9–50.9% of apoptotic cells resulted from the treatment of FTLEE at 0.4–1.0 mg/mL. In addition, only 7.1% of RMCCA-1 cells in the control underwent apoptosis. Note that the significant differences from the control were started at the 0.4 and 0.6 mg/mL-treated groups in HuCCA-1 and RMCCA-1 cells, respectively. In addition, 100 μ M of etoposide significantly increased the number of apoptotic cells in both HuCCA-1 and RMCCA-1 cells. These results suggest that apoptosis is the main mode of cell death induced by FTLEE in intrahepatic cholangiocarcinoma cells.

To explore the potential signaling pathways underlying FTLEE-induced HuCCA-1 and RMCCA-1 cell cycle arrest and apoptosis, the expression of the cell cycle regulatory protein, namely cyclin-D1, and apoptotic regulatory proteins, including Bcl-2 (anti-apoptot-

ic protein), caspase-3, Bax (proapoptotic protein), and PARP cleavage, were measured. Western immunoblots were performed on protein lysates of HuCCA-1 and RMCCA-1 cells treated with FTLEE at cytotoxic concentrations (0.2–1.2 mg/mL) for 24 h. The results showed that cyclin-D1, Bcl-2, and the inactive proenzyme form of caspase-3 were concentration-dependently reduced in FTLEE treatment (Fig. 7). Meanwhile, the proapoptotic protein Bax displayed upregulation in a concentration-dependent manner in FTLEE-treated cells. In addition, PARP, a 116 kDa nuclear enzyme, was cleaved to a fragment of 85 kDa in the FTLEE treatment. Taken together, these results confirmed that the FTLEE of *A. paniculata* altered the cell cycle process and activated the apoptotic signaling pathway in intrahepatic cholangiocarcinoma cells.

Discussion

A. paniculata has a broad range of pharmacological properties such as anti-inflammatory and anticancer activities. The present study showed that *A. paniculata* extracts strongly inhibited the growth of intrahepatic cholangiocarcinoma (HuCCA-1 and RMCCA-1) and hepatocellular carcinoma (HepG2 and SK-Hep1) cells. Since we found that only AP₁, not AP₃, AP₄, or AP₆, possessed a potent cytotoxic activity against these cancer cell lines, we speculated that AP₁, which is a major diterpenoid of *A. paniculata*, may play an important role on this cytotoxic effect of *A. paniculata* extracts. The IC₅₀ value of AP₁ at 24 h exposure in HepG2 cells in the present study (90.63 μ M) is very similar to that reported by Li and colleagues in 2007 (about 120 μ M) [16]. AP₁ was shown to possess potent cytotoxic activity on various cancer cell lines, such as KB (epidermoid leukemia) and P388 (lymphocytic leukemia) cells, whereas no such activity was observed for AP₃ and AP₄ [17]. It has been reported that AP₁ contained an α -alkylidene γ -butyrolactone moiety and three hydroxyls at C-3, C-19, and C-14, which are responsible for the cytotoxic activity against cancer cells [18]. Interestingly, *A. paniculata* extracts at different

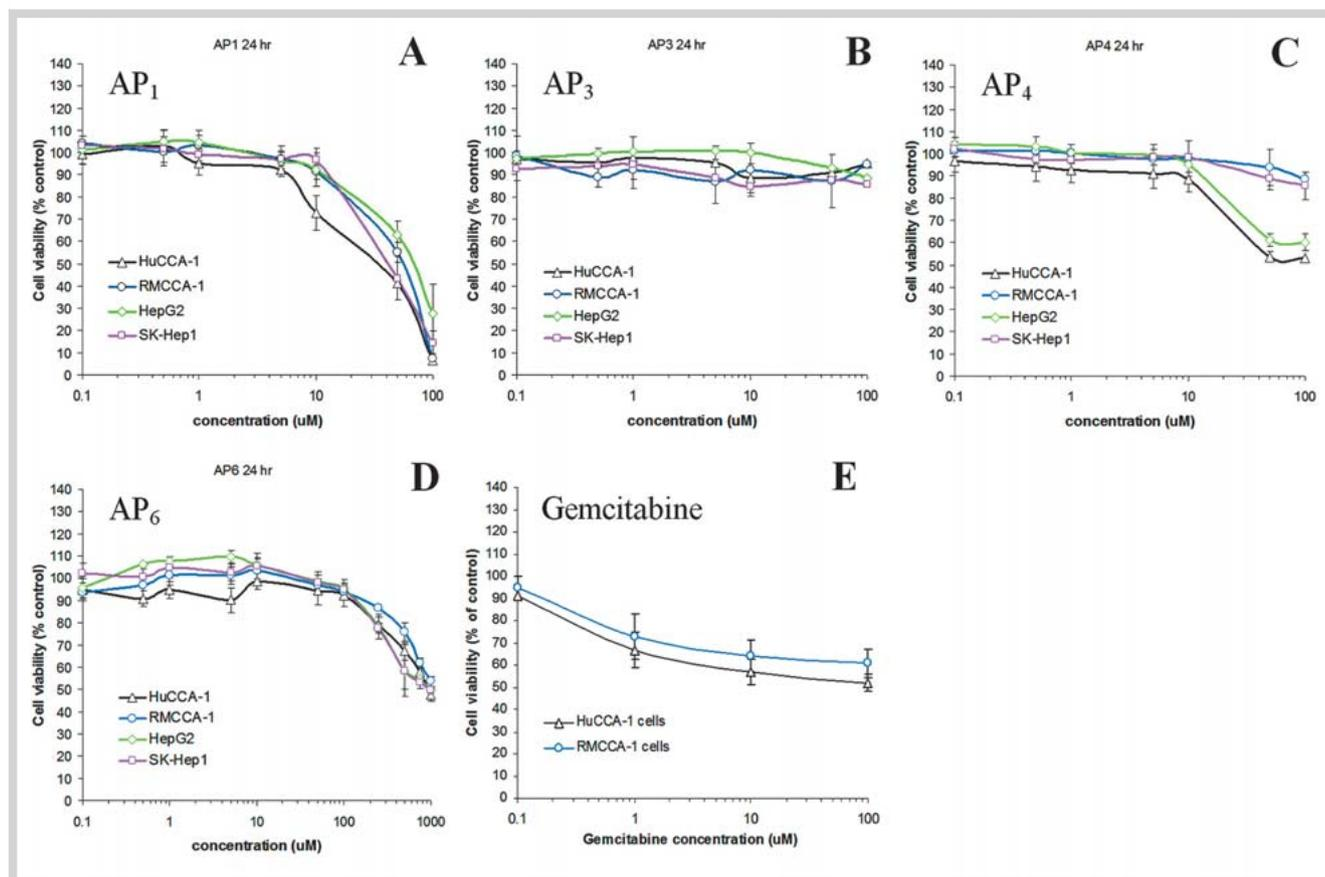


Fig. 4 The effects of pure diterpenoids including andrographolide (AP₁), 14-deoxy-11,12-didehydroandrographolide (AP₃), neoandrographolide (AP₄), and 14-deoxyandrographolide (AP₆) on hepatocellular carcinoma (HepG2 and SK-Hep1) and intrahepatic cholangiocarcinoma (HuCCA-1 and RMCCA-1) cell viability. Cells were treated with (A) 0.1–100 µM of AP₁, (B) 0.1–100 µM of AP₃, (C) 0.1–100 µM of AP₄, (D) 0.1–1000 µM of AP₆, or (E) 0.1–100 µM of gemcitabine (positive control) for 24 h. Cell viability was assessed by the MTT assay. Each data point represents the mean ± standard error of three independent experiments and is expressed as a relative value to control. (Color figure available online only.)

Diterpenoids	IC ₅₀ value at 24 h treatment (µM)			
	Hepatocellular carcinoma		Cholangiocarcinoma	
	HepG2	SK-Hep1	HuCCA-1	RMCCA-1
AP ₁	90.63	47.74	29.26	52.57
AP ₃	> 100	> 100	> 100	> 100
AP ₄	> 100	> 100	> 100	> 100
AP ₆	> 1000	> 1000	> 1000	> 1000

Table 3 Calculated IC₅₀ values of pure diterpenoids on hepatocellular and intrahepatic cholangiocarcinoma cells.

AP₁: andrographolide; AP₃: 14-deoxy-11,12-didehydroandrographolide; AP₄: neoandrographolide; AP₆: 14-deoxyandrographolide

plant growth stages which contained different contents of major diterpenoids exhibited different cytotoxic potency to cancer cells. The present study firstly showed that FTLEE, which contained a low amount of AP₁ but a high amount of AP₆, showed a more potent growth inhibiting effect to liver and bile duct cancer cells than MLWE, which contained a high amount of AP₁ but a low amount of AP₆. The cytotoxic effect of MLWE could be explained by the present amount of AP₁ while the cytotoxic effect of FTLEE could not. We hypothesized that the interaction between active diterpenoids, especially AP₁ and AP₆, may play a certain role in the growth inhibiting effect of FTLEE. Furthermore, other bioactive compounds that were present in the extracts apart from the four diterpenoids mentioned above may also contribute to this cytotoxic effect since more than 20 diterpenoids and 10 flavonoids had been identified in the ethanolic extract of *A. paniculata*

[8]. The HPLC chromatogram (● Fig. 2) indicates the unknown compounds in FTLEE (at retention times of 4.138, 4.681, and 5.048 min) which did not present in MLWE. It is possible that the other bioactive compounds in FTLEE may play a certain role on the inhibitory effects of cancer growth. Other ethanolic extract diterpenoids, for example, isoandrographolide, exhibited anti-proliferative activities to human leukemia HL-60 cells higher than AP₁ [19]. Furthermore, it has also been shown that some less abundant diterpenoids, including 14-acetylandrographolide, 3,19-isopropylideneandrographolide, and 14-deoxy-14,15-didehydroandrographolide, exhibited strong cytotoxic activities and induced cell cycle arrest against various types of cancer [20,21]. However, these hypotheses remain inconclusive and need further study.

Cell lines	Concentration of diterpenoids in the extracts at the IC ₅₀ value (μM)			
	AP ₁	AP ₃	AP ₄	AP ₆
Mature leaf water extract				
HepG2	91.92	7.27	51.45	25.65
SK-Hep1	61.28	4.85	34.30	17.10
HuCCA-1	37.71	2.98	21.11	10.52
RMCCA-1	75.42	5.97	42.21	21.05
First true leaf ethanol extract				
HepG2	1.62	16.58	12.66	353.06
SK-Hep1	0.93	9.50	7.26	203.47
HuCCA-1	0.67	6.91	5.28	147.98
RMCCA-1	1.21	12.43	9.50	266.36

Table 4 Concentrations of each diterpenoid in the extracts of *Andrographis paniculata* at the IC₅₀ value.

AP₁: andrographolide; AP₃: 14-deoxy-11,12-didehydroandrographolide; AP₄: neoandrographolide; AP₆: 14-deoxyandrographolide

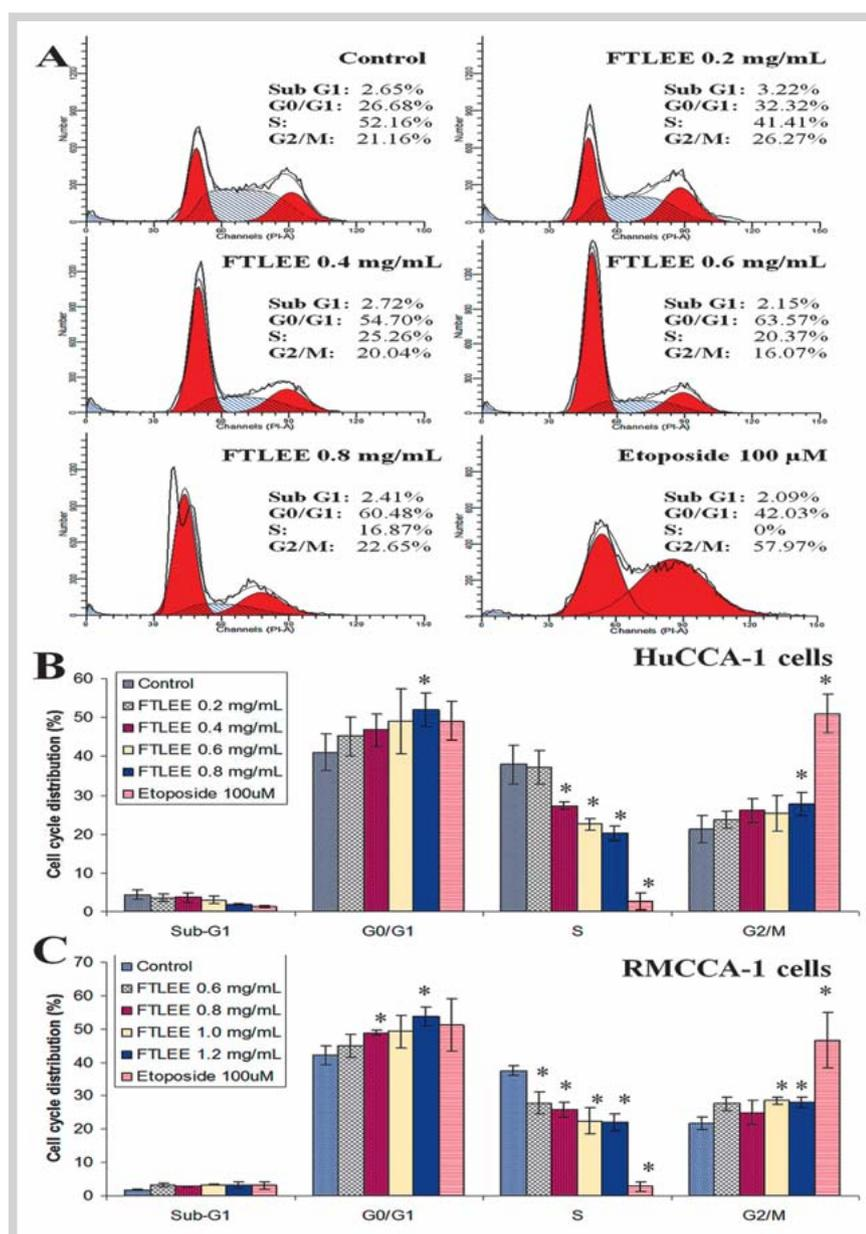


Fig. 5 The effects of the ethanolic extract of the first true leaf of *Andrographis paniculata* on the intrahepatic cholangiocarcinoma cell cycle. HuCCA-1 cells were treated with 0.2–0.8 mg/mL and RMCCA-1 cells were treated with 0.6–1.2 mg/mL of first true leaf ethanol extract (FTLEE) or 100 μM of etoposide (positive control) for 24 h and then subjected to flow cytometry with PI staining. **A** The representative histograms between PI intensity and cell numbers of HuCCA-1 cells. The cell cycle phase distribution of **(B)** HuCCA-1 cells and **(C)** RMCCA-1 cells after treatment with FTLEE. The data are the percentage mean of each cell cycle phase ± standard error of three independent experiments. * Represents a statistically significant difference from the controls at $p < 0.05$. (Color figure available online only.)

The difference in sensitivity among cancer cell lines to *A. paniculata* extracts or AP₁ has also been observed in this study. We also found that HuCCA-1 cells showed a twofold increase in

sensitivity to *A. paniculata* extracts or AP₁ than RMCCA-1 cells. Furthermore, it has been reported that AP₁ induced cytotoxic cell death in adenocarcinoma KKKU-M213 cells at

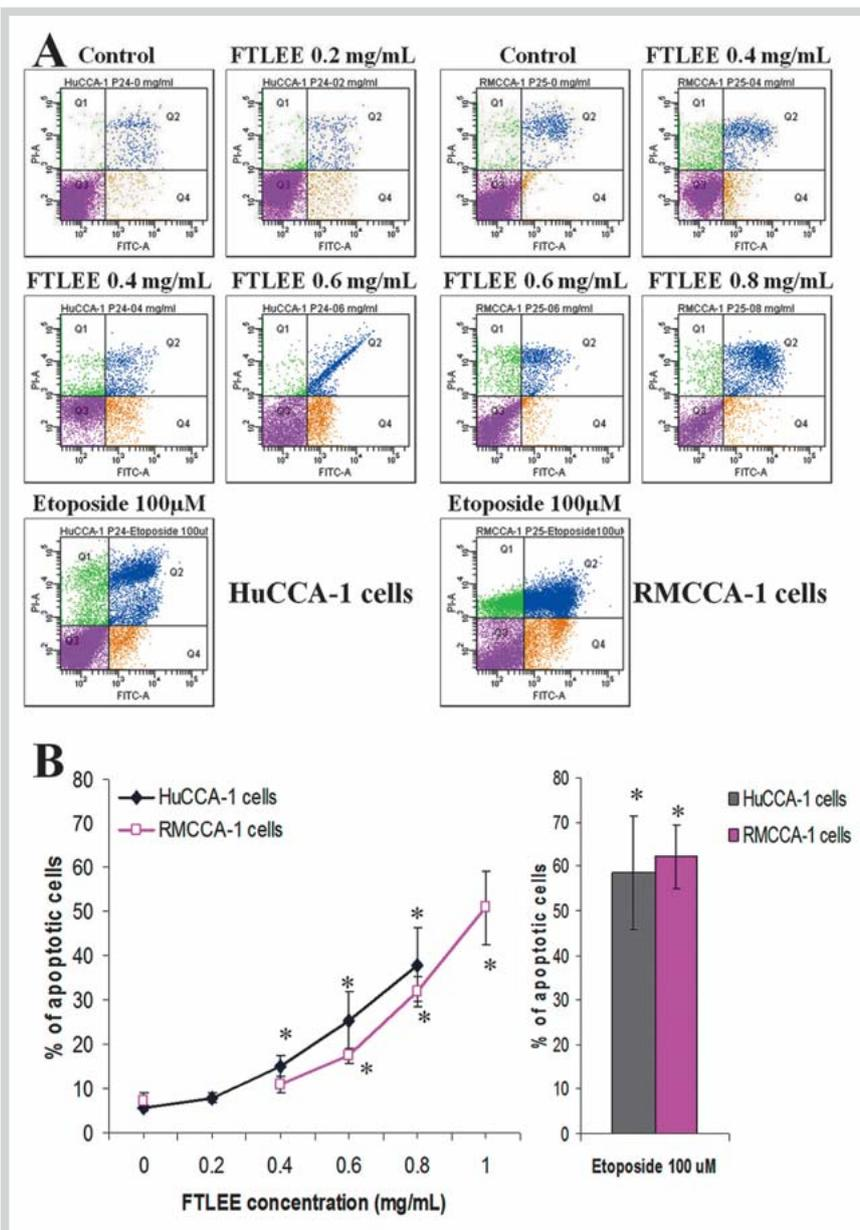


Fig. 6 Effects of the ethanolic extract of the first true leaf of *Andrographis paniculata* on intrahepatic cholangiocarcinoma cell apoptosis. HuCCA-1 and RMCCA-1 cells were treated with 0.2 – 1.0 mg/mL of FTLEE or 100 μ M of etoposide (positive control) for 24 h. Cell apoptosis was detected by flow cytometry with annexin-V-FITC/PI dual staining.

A The representative histograms of flow cytometric analysis using double staining with annexin-V-FITC (FITC-A) and PI (PI-A). Q1 (annexin-V⁻/PI⁺) is cells in necrosis; Q2 (annexin-V⁺/PI⁺) is cells in late apoptosis; Q3 (annexin-V⁻/PI⁻) is normal cells; Q4 (annexin-V⁺/PI⁻) is cells in early apoptosis. The percentage of apoptotic cells that include the cells in early apoptosis and late apoptosis \pm standard error of three independent experiments. * Represents a statistically significant difference from the control at $p < 0.05$. (Color figure available online only.)

24 h exposure with an IC_{50} value higher than 50 μ M [22], while our study showed that AP₁ induced cytotoxic cell death in HuCCA-1 cells with a lesser IC_{50} value (29.26 μ M). This could be explained, in part, to the difference in molecular characteristics of the different cancer cells. HuCCA-1 cells were established from a Thai cholangiocarcinoma patient with a chronic infection by liver fluke *Opisthorchis viverrini* [23], while there is no evidence of this parasite infection in RMCCA-1 cells [24]. Long-term liver fluke infection induced by chronic injury and inflammation of the biliary epithelium has been well recognized [25]. Moreover, we found that COX-2, which is a key inflammatory protein, was highly expressed in HuCCA-1 cells while it was detected lower in RMCCA-1 cells [unpublished data]. It has been reported that COX-2 specifically inhibited Fas-mediated apoptosis in cholangiocarcinoma KMBC cells and COX-2 inhibitor NS-398 restored Fas-mediated apoptosis in COX-2 transfected cells [26]. It is well documented that the anti-inflammatory activity of AP₁ occurred via the inhibition of COX-2 activity and expression [27]. All together, these suggest that the etiology of cancer cells, especially inflammation

background, could influence the anticancer properties of *A. paniculata* extracts and AP₁. However, this hypothesis remains inconclusive and warrants further study.

The present study also revealed that FTLEE increased cell cycle arrest and apoptosis in intrahepatic cholangiocarcinoma cells. This *A. paniculata* extract induced intrahepatic cholangiocarcinoma cell cycle arrest at the G₀/G₁ and G₂/M phases. The effect was likely due to the reduction of cyclin-D1 expression. Our observations are in line with previous studies which indicated that AP₁ induced cell cycle arrest at the G₀/G₁ or G₂/M phase in various cancer cell lines, for example, hepatoma cells (HepG2 and Hep3B) [16, 28], colorectal carcinoma Lovo cells [29], prostate cancer PC-3 cells [30], acute myeloid leukemic HL-60 cells [31], and lung adenocarcinoma CL1–5 cells [32]. Furthermore, a recent study demonstrated that the AP₁ analogue, which was modified from the parent compound by adding an epoxide moiety at the core structure C-17 and a silicon-based molecule, *tert*-butyldiphenylsilyl, at the C-19 side chain, induced adenocarcinoma KLU-M213 cell cycle arrest at the sub-G₀ and G₂/M phases

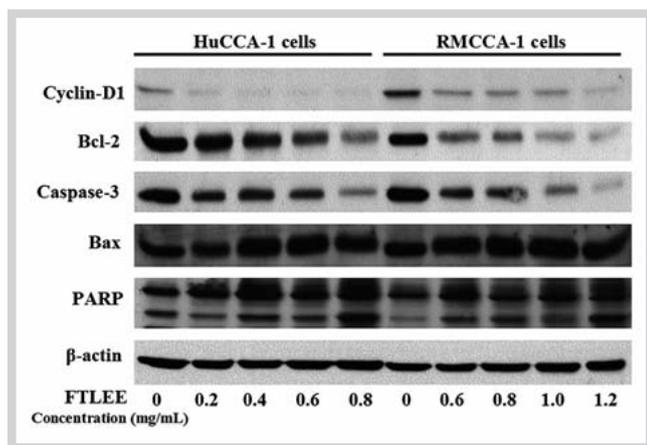


Fig. 7 Effects of the ethanolic extract of the first true leaf of *Andrographis paniculata* on cell cycle regulatory protein (cyclin-D1), anti-apoptotic protein (Bcl-2), proapoptotic proteins (caspase-3 and Bax), and poly (ADP-ribose) polymerase cleavage in intrahepatic cholangiocarcinoma cells. HuCCA-1 and RMCCA-1 cells were treated with 0.2–1.2 mg/mL of FTLEE for 24 h. Cyclin-D1, Bcl-2, caspase-3, Bax, and PARP cleavages were measured by Western immunoblot. β -actin was used to ensure an equal amount of loaded protein.

[22]. Our results also indicated that *A. paniculata* extract induced intrahepatic cholangiocarcinoma cell apoptosis. This effect was consistent with the downregulation of the key anti-apoptotic regulatory protein Bcl-2, upregulation of the crucial proapoptotic regulatory protein Bax, and reduction of the inactive proenzyme form of caspase-3 which plays a central role in the execution phase of cell apoptosis. These results are in agreement with our previous report and others which showed that AP₁ caused apoptosis by increasing the expression of p53, Bax, caspase-3, and decreasing the expression of Bcl-2 in various cancer cell lines such as neuroblastoma SK-N-SH [33], breast adenocarcinoma T47D and MDA-MB-231 [34, 35], melanoma B16F-10 [36], pancreatic cancer (AsPC-1, Panc-1, BxPC-3, SW1990, and Capan-1) [37], acute promyelocytic leukemia HL-60 and NB4 [31, 38], gastric cancer BGC-823 [39], hepatocellular carcinoma HepG2 and SMMC-7721 [35, 40], prostate carcinoma DU145, PzHPV-7, and PC-3 [41–43], cervical cancer HeLa [35], and lung adenocarcinoma CL1–5 [32] cells.

Our study revealed that the increasing concentration of *A. paniculata* treatment enhanced Bax protein expression and reduced the expression of Bcl-2 protein. Bax is one of the most important proapoptotic Bcl-2 family members promoting the mitochondrial apoptotic pathway, whereby it undergoes transformation and oligomerization to form pores in the outer mitochondrial membrane, leading to the release of proapoptotic proteins from mitochondria such as cytochrome C [44]. Bcl-2 is another important protein involved in the mitochondria-dependent apoptosis that has anti-apoptotic activity [45]. This suggests that an intrinsic mitochondria-dependent pathway might be involved in *A. paniculata*-induced cholangiocarcinoma apoptotic cell death. Numerous studies indicated that AP₁ promoted apoptosis in human cancer cells by affecting an intrinsic mitochondria-dependent pathway [30, 31, 35]. Furthermore, the reduction of the inactive proenzyme form of caspase-3 and cleavage of PARP were also observed in the present study, indicating that it was a caspase-dependent apoptosis. A recent study also revealed that AP₁ induced vascular smooth muscle cell apoptosis via ceramide-

p47phox-ROS and caspase-3 signaling cascade [46]. Notably, the intensities of the cleaved active forms of caspase-3 bands (17/19-kD) were very weak (data not shown). This may be due to the selected time point of FTLEE treatment not being suitable to detect these active caspase-3 forms since the two subunits of active caspase-3 are rapidly degraded and unstable from the ubiquitin-proteasome system [47]. Our results showed that cyclin-D1, which is a key regulator involved at the G0/G1 checkpoint, was reduced in *A. paniculata* treatment. Cyclin-D1 is an important transcriptional target of NF- κ B [48, 49]. Previous studies indicated that AP₁ and AP₃ potentially inhibited NF- κ B activation [50–53], which may be the reason leading to the reduction of cyclin-D1 in *A. paniculata* treatment.

In conclusion, this study revealed that *A. paniculata* potentially inhibited the growth of intrahepatic cholangiocarcinoma (HuCCA-1 and RMCCA-1) cells. Indeed, this growth inhibiting effect of *A. paniculata* was caused by the induction of cell cycle arrest and apoptosis. All together, this study suggests that *A. paniculata* and its major bioactive compounds, such as AP₁, may be a promising candidate for bile duct cancer treatment. In light of the lack of effective therapeutic options for bile duct cancer, *A. paniculata* is an herbal treatment option that is worthy of consideration for further research. Further *in vivo* studies using an animal model such as a tumor xenograft nude mouse model for a cholangiocarcinoma study may be used to confirm the present *in vitro* results of FTLEE as an anticancer drug and provide more physiological relevant evidence.

Materials and Methods

Chemicals and standard pure diterpenoids

Andrographolide (AP₁, purity 98%), gemcitabine hydrochloride (purity \geq 98%) and etoposide (purity \geq 98%) were purchased from Sigma-Aldrich. Another three diterpenoids, namely, 14-deoxy-11,12-didehydroandrographolide (AP₃, purity 96%), neoandrographolide (AP₄, purity 99%), and 14-deoxyandrographolide (AP₆, purity 99%), were isolated and purified in-house from *A. paniculata* according to our previous report [4].

Preparation of *Andrographis paniculata* extracts

A. paniculata plants were identified by Dr. Wongsatit Chuakul and a voucher specimen was deposited at the Pharmaceutical Botany Mahidol Herbarium, Department of Pharmaceutical Botany, Faculty of Pharmacy, Mahidol University, Bangkok, Thailand (PBM 3760). Two dried *A. paniculata* raw materials were selected. One was the aerial part of *A. paniculata* at the 50% flowering stage (mature leaf stage) harvested from Nakornpathom Province, Thailand. Another one was the aerial part of *A. paniculata* at the first true leaf stage harvested from the greenhouse at the Chulabhorn Research Institute, Bangkok. Plant materials were washed and then dried in an oven at 35–45 °C. The dried plant materials were ground into a powder using a blender (Waring Commercial) and kept at room temperature until extraction. For MLWE, 3 kg of aerial parts at the 50% flowering stage of *A. paniculata* were extracted with 15 L of hot water (70–75 °C) for 30 min. The extract was then filtered and collected. The residue was re-extracted twice with 15 L of hot water each time. The combined water extracts were concentrated by using a spray dry method. For another *A. paniculata* extract, the FTLEE was prepared by extracting 4.1 g of first true leaf stage powder in 80 mL ethanol. The residue was re-extracted twice with 80 mL ethanol

each time. The combined ethanol extracts were concentrated by using a rotary evaporator at a temperature of $< 50^{\circ}\text{C}$.

Chromatographic analysis of *Andrographis paniculata* extracts

Twenty-five milligrams of MLWE were dissolved in 2.0 mL of hot water ($70\text{--}75^{\circ}\text{C}$) and vigorously shaken (two replicates per sample). The extract solutions were left at room temperature until they cooled down. The FTLEE was accurately weighed (7.04 mg, two replicates per sample) and then dissolved in 1.0 mL methanol. The dissolved extract solutions were filtered through a 0.45- μm nylon membrane (Chrom Tech) prior to HPLC analysis. The four active diterpenoids, namely AP₁, AP₃, AP₄, and AP₆, in the extracts of *A. paniculata* were analyzed simultaneously by HPLC-DAD (Agilent Technologies) on a reverse-phase column (Zorbax SB-C18; $4.6 \times 75\text{ mm}$, $3.5\ \mu\text{m}$) connected to a cartridge guard column (Agilent Technologies), according to our previous study [9]. Briefly, the mobile phase consisted of 28% acetonitrile in water with a flow rate of 1.2 mL/min. The temperature of the column was controlled at 25°C and the detection with the diode array detector (DAD; Model G1315A, Agilent Technologies) at 205 nm. The injection volume was 5 μL . A standard mixture containing AP₁, AP₃, AP₄, and AP₆ in methanol was prepared in the range of 0.5–1000 $\mu\text{g}/\text{mL}$. The peak area of each compound was plotted against the concentration.

Cell culture

The human intrahepatic cholangiocarcinoma cell lines, including HuCCA-1 and RMCCA-1, derived from epithelial bile duct tumor masses of Thai cholangiocarcinoma patients were established and kindly provided by Prof. Stitaya Sirisinha [23] and Dr. Kavin Leelawat [24], respectively. HuCCA-1 and RMCCA-1 cells were cultured in HAM's F-12 medium (Gibco) supplemented with 2 mM L-glutamine (Gibco), 100 units/mL P/S (Gibco), and 10% (v/v) FBS (JR Scientific, Woodland). Liver cancer cell lines, including the Hep-G2 cell line (a human epithelial hepatocellular carcinoma) and SK-Hep1 (a human liver adenocarcinoma), were purchased from ATCC (Rockville). Hep-G2 cells were cultured in minimum essential medium Eagle (Gibco) supplemented with 2 mM L-glutamine, 1.0 mM sodium pyruvate (Sigma-Aldrich), 0.1 mM nonessential amino acids (Sigma-Aldrich), 100 unit/mL P/S, and 10% FBS. SK-Hep1 cells were grown in RPMI 1640 medium (Gibco) containing 2 mM L-glutamine, 100 unit/mL P/S, and 10% FBS. All cells were maintained at 37°C in a saturated humidity atmosphere containing 95% air and 5% CO_2 .

Cell viability assay

Cell viability was measured by a quantitative colorimetric assay with MTT (3-(4,5-dimethylthiazol-2-yl)-2,5-diphenyl-tetrazolium bromide) (Sigma-Aldrich) showing the mitochondrial activity of living cells. Cells were seeded in a 96-well plate (1×10^4 cells/well) and cultured overnight for attachment. The next day, the cells were treated with various concentrations of *A. paniculata* extracts (MLWE or FTLEE), its bioactive compounds (AP₁, AP₃, AP₄, or AP₆), or gemcitabine (positive control) for 24 h. At the end of the respective incubation period, the media were removed and then 100 μL of MTT (500 $\mu\text{g}/\text{mL}$ MTT in media) were added per well, followed by the incubation of the plate for 4 h at 37°C for color development. Then, MTT was removed and the cells were lysed with DMSO (Sigma-Aldrich). Following solubilization, the absorbance at 570 nm was measured using a microplate scanning spectrophotometer (SpectraMax M3, Molecular Devices).

Apoptosis assay

Cells (5×10^6 cells) were seeded in a 100-mm plate and cultured overnight for attachment. The next day, the cells were treated with various concentrations of *A. paniculata* extract or 100 μM of etoposide (positive control) for 24 h. The PS externalization on apoptotic cells was detected by an annexin V-FITC apoptosis detection kit (BD Biosciences). In brief, at the end of the incubation period, the medium was removed, cells were collected with trypsin (Gibco), and the supernatant was removed by centrifugation at $500 \times g$, 4°C for 5 min. Cell pellets were washed twice with PBS (Gibco), then resuspended in annexin-V binding buffer (0.01 M HEPES/NaOH, pH 7.4, 0.15 mM NaCl, 2.5 mM CaCl_2), followed by staining at room temperature in the dark with 5 $\mu\text{g}/\text{mL}$ of annexin-V-FITC and PI for 15 min. The stained cells were analyzed by the flow cytometer BD FACSCanto (Becton Dickinson). Green fluorescence (530/42 nm), indicative of the annexin-V-FITC binding of apoptotic cells, and red fluorescence (585/42 nm), indicative of PI uptake by damaged cells, were evaluated using logarithmic amplification and electronic compensation for spectral overlap. The amount of early apoptosis, late apoptosis, and necrosis was measured as the percentage of annexin-V positive/PI negative, annexin-V positive/PI positive, and annexin-V negative/PI positive cells, respectively.

Cell cycle assay

Cells (5×10^6 cells) were seeded in a 100-mm plate and cultured overnight for attachment. The next day, the cells were treated with various concentrations of *A. paniculata* extracts or 100 μM of etoposide (positive control). After 24 h incubation, the cells were analyzed for the distribution of sub-G1, G0/G1, G2/M, and S phases of the cell cycle by flow cytometry with PI staining. Briefly, the medium was removed and the cells were harvested with trypsin, and then the supernatant was removed by centrifugation at $500 \times g$, 4°C for 5 min. Cell pellets were washed with PBS and fixed in 70% ethanol overnight at -20°C . Then the cells were washed with cold PBS and stained with PI solution [50 $\mu\text{g}/\text{mL}$ PI (Sigma-Aldrich) and 0.5 $\mu\text{g}/\text{mL}$ RNase (Sigma-Aldrich) in PBS] at an ambient temperature for 15 min. The cell cycle stages were measured by flow cytometry and the data was analyzed by Modfit LT software (Verity House Software).

Western immunoblotting assay

The cells (5×10^6 cells) were seeded in a 100-mm plate and cultured overnight for attachment. The next day, the cells were treated with various concentrations of *A. paniculata* extracts. After 24 h incubation, the medium was removed and the cells were harvested with trypsin, and the supernatant was removed by centrifugation at $500 \times g$, 4°C for 5 min. Cells were lysed in lysis buffer containing 10 mM Tris-HCl, pH 7.4, 150 mM NaCl, 1% triton X-100, 1 mM PMSF, 1 mM Na_3VO_4 , 20 mM NaF, and 1 \times protease inhibitor cocktail set I (Calbiochem). Cell lysates were sonicated and incubated at 4°C for 30 min and then centrifuged at $16000 \times g$ for 15 min at 4°C . The concentration of protein was determined by the Bradford assay (Bio-Rad, Hercules). The protein (50 μg) was mixed with Laemmli loading buffer (62.5 mM Tris-HCl, pH 6.8, 25% glycerol, 2% SDS, 0.01% bromophenol blue, and 5% 2-mercaptoethanol) and boiled at 95°C for 5 min. The proteins were separated by 7.5% SDS-polyacrylamide gel electrophoresis in a Mini-PROTEAN II system (Bio-Rad). The separated protein bands were transferred onto a nitrocellulose membrane (GE Healthcare). The membrane was incubated in blocking buffer containing 5% nonfat dry milk in TBST buffer (10 mM Tris-HCl,

pH 8.0, 150 mM NaCl, and 0.05% Tween-20) for 1 h at room temperature followed by overnight incubation at 4°C with the primary antibody. The antibodies against cyclin D1, Bcl-2, Bax, caspase-3, and β -actin were obtained from Cell Signaling Technology (Cell Signaling). The PARP antibody was purchased from BD Biosciences. After washing with TBST buffer, the membrane was incubated with horseradish-peroxidase conjugated secondary antibodies (GE Healthcare) for 2 h at room temperature. The protein bands stained by the antibody were visualized by using enhanced chemiluminescence (GE Healthcare) followed by exposure to X-ray films (Pierce/Perbio). Relative protein expressions were calculated from band intensities using computerized densitometry with ImageQuantTL software (GE Healthcare).

Statistical analysis

Data are expressed as means \pm standard errors of three independent experiments. A statistically significant difference was assessed by the Student's t-test. A two-tailed p value less than 0.05 was considered a statistically significant difference.

Acknowledgments

This study was supported by a research grant from the Chulabhorn Research Institute. The authors kindly acknowledge Mr. Likhit Suchikran for providing *A. paniculata* seeds and mature leaf materials. We would like to express our great appreciation to Mr. Supachai Ritruethai and Mrs. Jittra Saehun for their assistance on plant cultivation and extraction. We also thank Ms. Kanjana Chaiyot for her technical assistance with cell cultures. Results from this work were already submitted for a petty patent in Thailand (request No. 1203001500, December 27, 2012; status: pending).

Conflict of Interest

The authors declare that there is no known conflict of interest with any organization regarding the materials discussed in this manuscript.

References

- Akbar S. *Andrographis paniculata*: a review of pharmacological activities and clinical effects. *Altern Med Rev* 2011; 16: 66–77
- Dey YN, Kumari S, Ota S, Srikanth N. Phytopharmacological review of *Andrographis paniculata* (Burm.f) Wall. ex Nees. *Int J Nutr Pharmacol Neurol Dis* 2013; 3: 3–10
- Lim JC, Chan TK, Ng DS, Sagineedu SR, Stanslas J, Wong WS. Andrographolide and its analogues: versatile bioactive molecules for combating inflammation and cancer. *Clin Exp Pharmacol Physiol* 2011; 39: 300–310
- Pholphana N, Rangkadilok N, Thongnest S, Ruchirawat S, Ruchirawat M, Satayavivad J. Determination and variation of three active diterpenoids in *Andrographis paniculata* (Burm.f.) Nees. *Phytochem Anal* 2004; 15: 365–371
- Rajagopal S, Kumar RA, Deevi DS, Satyanarayana C, Rajagopalan R. Andrographolide, a potential cancer therapeutic agent isolated from *Andrographis paniculata*. *J Exp Ther Oncol* 2003; 3: 147–158
- Yoopan N, Thisoda P, Rangkadilok N, Sahasitawat S, Pholphana N, Ruchirawat S, Satayavivad J. Cardiovascular effects of 14-deoxy-11, 12-didehydroandrographolide and *Andrographis paniculata* extracts. *Planta Med* 2007; 73: 503–511
- Thisoda P, Rangkadilok N, Pholphana N, Worasuttayangkurn L, Ruchirawat S, Satayavivad J. Inhibitory effect of *Andrographis paniculata* extract and its active diterpenoids on platelet aggregation. *Eur J Pharmacol* 2006; 553: 39–45
- Chao WW, Lin BF. Isolation and identification of bioactive compounds in *Andrographis paniculata* (Chuanxinlian). *Chin Med* 2010; 5: 17
- Pholphana N, Rangkadilok N, Saehun J, Ritruethai S, Satayavivad J. Changes in the contents of four active diterpenoids at different growth stages in *Andrographis paniculata* (Burm.f.) Nees (Chuanxinlian). *Chin Med* 2013; 8: 2
- Sripa B, Pairojkul C. Cholangiocarcinoma: lessons from Thailand. *Curr Opin Gastroenterol* 2008; 24: 349–356
- Shin HR, Oh JK, Masuyer E, Curado MP, Bouvard V, Fang Y, Wiangnon S, Sripa B, Hong ST. Comparison of incidence of intrahepatic and extrahepatic cholangiocarcinoma – focus on East and South-Eastern Asia. *Asian Pac J Cancer Prev* 2011; 11: 1159–1166
- Khan SA, Toledano MB, Taylor-Robinson SD. Epidemiology, risk factors, and pathogenesis of cholangiocarcinoma. *HPB (Oxford)* 2008; 10: 77–82
- de Martel C, Plummer M, Franceschi S. Cholangiocarcinoma: descriptive epidemiology and risk factors. *Gastroenterol Clin Biol* 2010; 34: 173–180
- Charbel H, Al-Kawas FH. Cholangiocarcinoma treatment. *Curr Gastroenterol Rep* 2012; 14: 528–533
- Khan SA, Davidson BR, Goldin RD, Heaton N, Karani J, Pereira SP, Rosenberg WM, Tait P, Taylor-Robinson SD, Thillainayagam AV, Thomas HC, Wasan H. Guidelines for the diagnosis and treatment of cholangiocarcinoma: an update. *Gut* 2012; 61: 1657–1669
- Li J, Cheung HY, Zhang Z, Chan GK, Fong WF. Andrographolide induces cell cycle arrest at G2/M phase and cell death in HepG2 cells via alteration of reactive oxygen species. *Eur J Pharmacol* 2007; 568: 31–44
- Siripong P, Kongkathip B, Preechanukool K, Picha P, Tunsuwan K, Taylor WC. Cytotoxic diterpenoid constituents from *Andrographis paniculata* Nees. *leaves. ScienceAsia* 1992; 18: 187–194
- Varma A, Padh H, Shrivastava N. Andrographolide: a new plant-derived antineoplastic entity on horizon. *Evid Based Complement Alternat Med* 2011; 2011: 815390
- Chen L, Zhu H, Wang R, Zhou K, Jing Y, Qiu F. ent-Labdane diterpenoid lactone stereoisomers from *Andrographis paniculata*. *J Nat Prod* 2008; 71: 852–855
- Jada SR, Subur GS, Matthews C, Hamzah AS, Lajis NH, Saad MS, Stevens MF, Stanslas J. Semisynthesis and *in vitro* anticancer activities of andrographolide analogues. *Phytochemistry* 2007; 68: 904–912
- Geethangili M, Rao YK, Fang SH, Tzeng YM. Cytotoxic constituents from *Andrographis paniculata* induce cell cycle arrest in jurkat cells. *Phytother Res* 2008; 22: 1336–1341
- Nateewattana J, Dutta S, Reabroi S, Saeeng R, Kasemsook S, Chairoungdua A, Weerachayaphorn J, Wongkham S, Piyachaturawat P. Induction of apoptosis in cholangiocarcinoma by an andrographolide analogue is mediated through topoisomerase II alpha inhibition. *Eur J Pharmacol* 2013; 723 C: 148–155
- Sirisinha S, Tengchaisri T, Boonpucknavig S, Prempracha N, Ratanarapee S, Pausawasdi A. Establishment and characterization of a cholangiocarcinoma cell line from a Thai patient with intrahepatic bile duct cancer. *Asian Pac J Allergy Immunol* 1991; 9: 153–157
- Rattanasinganchan P, Leelawat K, Treepongkaruna SA, Tocharoentana-phol C, Subwongcharoen S, Suthiphongchai T, Tohtong R. Establishment and characterization of a cholangiocarcinoma cell line (RMCCA-1) from a Thai patient. *World J Gastroenterol* 2006; 12: 6500–6506
- Sripa B, Kaewkes S, Sithithaworn P, Mairiang E, Laha T, Smout M, Pairojkul C, Bhudhisawasdi V, Tesana S, Thinkamrop B, Bethony JM, Loukas A, Brindley PJ. Liver fluke induces cholangiocarcinoma. *PLoS Med* 2007; 4: e201
- Nzeako UC, Guicciardi ME, Yoon JH, Bronk SF, Gores GJ. COX-2 inhibits Fas-mediated apoptosis in cholangiocarcinoma cells. *Hepatology* 2002; 35: 552–559
- Hidalgo MA, Romero A, Figueroa J, Cortes P, Concha II, Hancke JL, Burgos RA. Andrographolide interferes with binding of nuclear factor-kappaB to DNA in HL-60-derived neutrophilic cells. *Br J Pharmacol* 2005; 144: 680–686
- Shen KK, Liu TY, Xu C, Ji LL, Wang ZT. Andrographolide inhibits hepatoma cells growth and affects the expression of cell cycle related proteins. *Yao Xue Xue Bao* 2009; 44: 973–979
- Shi MD, Lin HH, Lee YC, Chao JK, Lin RA, Chen JH. Inhibition of cell-cycle progression in human colorectal carcinoma Lovo cells by andrographolide. *Chem Biol Interact* 2008; 174: 201–210
- Wong HC, Sagineedu SR, Lajis NH, Loke SC, Stanslas J. Andrographolide induces cell cycle arrest and apoptosis in PC-3 prostate cancer cells. *Afr J Pharm Pharmacol* 2011; 5: 225–233

- 31 Cheung HY, Cheung SH, Li J, Cheung CS, Lai WP, Fong WF, Leung FM. Andrographolide isolated from *Andrographis paniculata* induces cell cycle arrest and mitochondrial-mediated apoptosis in human leukemic HL-60 cells. *Planta Med* 2005; 71: 1106–1111
- 32 Lai YH, Yu SL, Chen HY, Wang CC, Chen HW, Chen JJ. The HLJ1-targeting drug screening identified Chinese herb andrographolide that can suppress tumour growth and invasion in non-small-cell lung cancer. *Carcinogenesis* 2013; 34: 1069–1080
- 33 Thiantanawat A, Watcharasi P, Ruchirawat S, Satayavivad J. Modulation of cell cycle and apoptosis signaling by the three active diterpenoids from *Andrographis paniculata* Nees. In: Abstract Book of the fifth Princess Chulabhorn International Science Congress: evolving genetics and its global impact. Bangkok: Amarin Printing and Publishing Company Limited; 2004: 57
- 34 Sukardiman H, Widayawaryanti A, Sismindari, Zaini NC. Apoptosis inducing effect of andrographolide on TD-47 human breast cancer cell line. *Afr J Tradit Complement Altern Med* 2007; 4: 345–351
- 35 Zhou J, Zhang S, Ong CN, Shen HM. Critical role of pro-apoptotic Bcl-2 family members in andrographolide-induced apoptosis in human cancer cells. *Biochem Pharmacol* 2006; 72: 132–144
- 36 Pratheeshkumar P, Sheeja K, Kuttan G. Andrographolide induces apoptosis in B16F-10 melanoma cells by inhibiting NF-kappaB-mediated bcl-2 activation and modulating p53-induced caspase-3 gene expression. *Immunopharmacol Immunotoxicol* 2011; 34: 143–151
- 37 Bao GQ, Shen BY, Pan CP, Zhang YJ, Shi MM, Peng CH. Andrographolide causes apoptosis via inactivation of STAT3 and Akt and potentiates antitumor activity of gemcitabine in pancreatic cancer. *Toxicol Lett* 2013; 222: 23–35
- 38 Manikam SD, Stanslas J. Andrographolide inhibits growth of acute promyelocytic leukaemia cells by inducing retinoic acid receptor-independent cell differentiation and apoptosis. *J Pharm Pharmacol* 2009; 61: 69–78
- 39 Li SG, Shao QS, Wang YY, Peng T, Zhao YF, Yang YJ, Huang D. Effect of andrographolide on proliferation and apoptosis of gastric cancer BGC-823 cells. *Zhonghua Wei Chang Wai Ke Za Zhi* 2013; 16: 676–680
- 40 Yang L, Wu D, Luo K, Wu S, Wu P. Andrographolide enhances 5-fluorouracil-induced apoptosis via caspase-8-dependent mitochondrial pathway involving p53 participation in hepatocellular carcinoma (SMMC-7721) cells. *Cancer Lett* 2009; 276: 180–188
- 41 Zhang ZR, Al Zaharna M, Wong MM, Chiu SK, Cheung HY. Taxifolin enhances andrographolide-induced mitotic arrest and apoptosis in human prostate cancer cells via spindle assembly checkpoint activation. *PLoS One* 2013; 8: e54577
- 42 Zhao F, He EQ, Wang L, Liu K. Anti-tumor activities of andrographolide, a diterpene from *Andrographis paniculata*, by inducing apoptosis and inhibiting VEGF level. *J Asian Nat Prod Res* 2008; 10: 467–473
- 43 Chun JY, Tummala R, Nadiminty N, Lou W, Liu C, Yang J, Evans CP, Zhou Q, Gao AC. Andrographolide, an herbal medicine, inhibits interleukin-6 expression and suppresses prostate cancer cell growth. *Genes Cancer* 2010; 1: 868–876
- 44 Schafer B, Quispe J, Choudhary V, Chipuk JE, Ajero TG, Du H, Schneider R, Kuwana T. Mitochondrial outer membrane proteins assist Bid in Bax-mediated lipidic pore formation. *Mol Biol Cell* 2009; 20: 2276–2285
- 45 Cory S, Adams JM. The Bcl2 family: regulators of the cellular life-or-death switch. *Nat Rev Cancer* 2002; 2: 647–656
- 46 Chen YY, Hsu MJ, Sheu JR, Lee LW, Hsieh CY. Andrographolide, a novel NF-kappaB inhibitor, induces vascular smooth muscle cell apoptosis via a ceramide-p47phox-ROS signaling cascade. *Evid Based Complement Alternat Med* 2013; 2013: 821813
- 47 Chen L, Smith L, Wang Z, Smith JB. Preservation of caspase-3 subunits from degradation contributes to apoptosis evoked by lactacystin: any single lysine or lysine pair of the small subunit is sufficient for ubiquitination. *Mol Pharmacol* 2003; 64: 334–345
- 48 Joyce D, Albanese C, Steer J, Fu M, Bouzahzah B, Pestell RG. NF-kappaB and cell-cycle regulation: the cyclin connection. *Cytokine Growth Factor Rev* 2001; 12: 73–90
- 49 Guttridge DC, Albanese C, Reuther JY, Pestell RG, Baldwin jr. AS. NF-kappaB controls cell growth and differentiation through transcriptional regulation of cyclin D1. *Mol Cell Biol* 1999; 19: 5785–5799
- 50 Chao WW, Kuo YH, Lin BF. Anti-inflammatory activity of new compounds from *Andrographis paniculata* by NF-kappaB transactivation inhibition. *J Agric Food Chem* 2010; 58: 2505–2512
- 51 Luo W, Liu Y, Zhang J, Luo X, Lin C, Guo J. Andrographolide inhibits the activation of NF-kappaB and MMP-9 activity in H3255 lung cancer cells. *Exp Ther Med* 2013; 6: 743–746
- 52 Wang LJ, Zhou X, Wang W, Tang F, Qi CL, Yang X, Wu S, Lin YQ, Wang JT, Geng JG. Andrographolide inhibits oral squamous cell carcinogenesis through NF-kappaB inactivation. *J Dent Res* 2013; 90: 1246–1252
- 53 Zhu T, Wang DX, Zhang W, Liao XQ, Guan X, Bo H, Sun JY, Huang NW, He J, Zhang YK, Tong J, Li CY. Andrographolide protects against LPS-induced acute lung injury by inactivation of NF-kappaB. *PLoS One* 2013; 8: e56407